Numerical and Experimental Investigation of SPH, SPG, and FEM for High-Velocity Impact Applications

Marvin Becker[1], Marina Seidl[1], Miriam Mehl[2], M'hamed Souli[3], Jean-François Legendre[1]

[1]ISL (Institute of Saint-Louis)
[2]University of Stuttgart
[3]Lille University

During a high-velocity impact event large pressure, strain rate, and deformation occur. This is a very demanding scenario for mesh-based approaches like the FEM (Finite Element Method). In particular, for the description of fracture, special techniques like erosion or node splitting are required. For a comprehensive validation, we have designed a projectile surrogate and conducted impact experiments at different oblique angles in our laboratories. These experiments are observed with X-ray cinematography and physical properties for validation are extracted from the images. For the highly dynamic behavior during the impact, an alternative to mesh-based approaches are particle-based methods. LS-DYNA® offers two pure particle methods, SPH (Smooth Particle Hydrodynamics) and SPG (Smooth Particle Galerkin). This study compares SPH to the FEM results and the experimental data.
Since the discretization requirements for the numerical approaches are different, it is not possible to compare exactly the same discretization. Instead, the number of nodes is chosen similarly. The accuracy is investigated qualitatively, using X-ray images, as well as quantitatively, using the extracted properties from the experiments.

1 Introduction

The impact of a projectile has been investigated by a broad community [1, 2, 3, 4, 5]. For academic research, the application serves as a validation case for the effectiveness of their methods with respect to large pressures and strain rates [6]. For the military, it is used to determine the efficiency of protective structures. They are interested in the response of different materials like steel, composite or ceramic, each of them requiring a different material model.
For small deformations and little material erosion (e.g. Taylor tests), the classical Lagrangian-FEM approach can be applied without major modifications. However, for higher velocities, the numerical material erosion increases and energy and mass are not preserved anymore. Thus, the simulation results do not always coincide with experimental results anymore. Therefore, LS-DYNA® [7] introduces a few workarounds: **`MAT_ADD_EROSION`** can be used to tune the model. The choice of erosion criteria is most often not physically argued. Instead, it is chosen, such that the particular scene of interest is described nicely. If the same model would be applied to a different impact scenario (in terms of projectile shape, impact velocity, or oblique angle) it would not be predictive and would have to be tuned for the new case again. Another option is **`ADAPTIVE_SOLID_TO_SPH.`** It conserves energy and mass since elements are not eroded but transferred to SPH-particles if the element fails. Both options were introduced to treat the shortcomings of the FEM in this application. Changing the whole model to a different technique, like SPH or SPG, requires a completely different preprocessing. Further, the Lagrangian FEM is a very reliable and well-understood method if no large deformations occur. Thus, the general aim is to stick to FE as long as possible and use particle methods only when required.
Our aim is to compare the different numerical descriptions available in LS-DYNA® for the high velocity impact of a projectile surrogate against an armor steel plate under different oblique angles.

2 Application and Experimental Results

The application is a very simplified test case, which is designed to fulfill two properties: On the one hand, it is supposed to be easy to set up in the numerical experiments. Therefore, the surrogate has a simplified geometry and consists of only one material of characterized steel. On the other hand, the experiments should contain little uncertainties due to yawing. Hence, the surrogate is designed with a round-shaped nose. The experiments are observed with X-ray cinematography and then evaluated quantitatively and qualitatively.

2.1 Case Description

A *7.62mm* projectile surrogate impacts an armor steel plate at a velocity of *800m/s*. Our primary interest is not the perforation efficiency but the fracture behavior of the impactor itself. Hence, the study covers the whole range of obliquity angles.
This study validates the numerical methods implemented in LS-DYNA® with respect to oblique high-velocity impact and the associated fragmentation behavior. The paper benchmarks different methods and considers the two angles of 30 and 75 degrees.

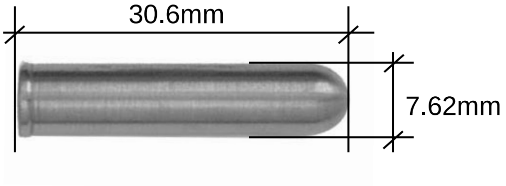

Figure 1: The case study is conducted for a 7.62mm surrogate with an L/D ratio of 4 made of M300 armor steel.

2.2 Experimental Setup / Methodology

The experiments for this paper are conducted in the laboratories at ISL[1]. Figure 2 explains the setup: A clamping device for setting up the oblique impact was designed and a new observation approach (Multi-anode X-ray cinematography [8]) was required for observing the qualitative dynamic behavior in this challenging application. Dust and high-energetic lightning during the impact hides the action to optical sensors and requires this advanced imaging technique. Fortunately, this new setup produces separate images which give the opportunity to extract quantitative results and to compare them to the simulation output. This was not possible for a multiple-exposed X-ray image which is the standard approach for this kind of application.
Angles between 0 and 75 degrees are investigated with an incremental angle of 15 degrees. Each experiment is repeated at least twice. The yawing of the projectile during the impact is measured optically for each experiment. Experiments with more than five degrees yawing are discarded.
The raw images contain noise and parallax error. To capture the dynamic behavior and extract physical properties with best accuracy, a software was developed by the author to do the alignment and detect the fragments (compare Figure 3).

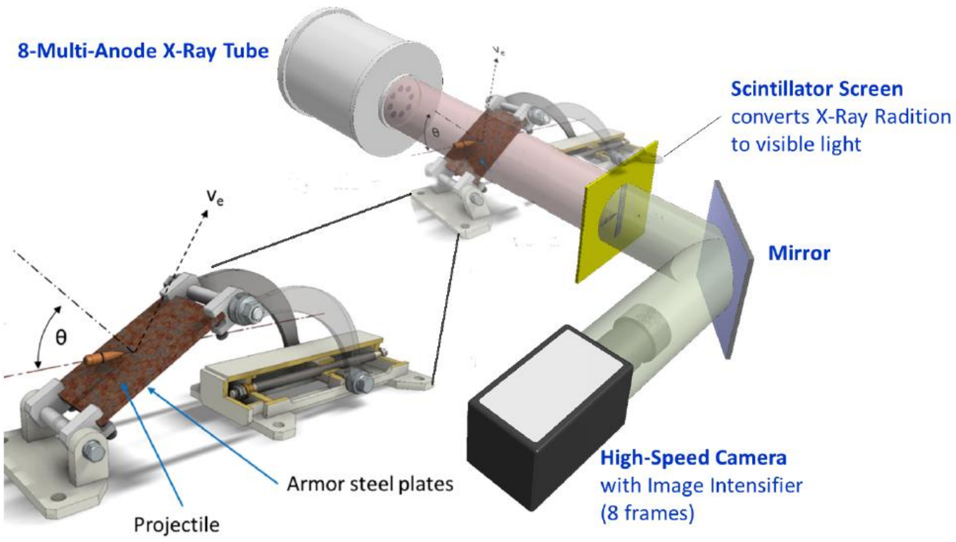

Figure 2: Left part: Clamping device for oblique impact experiments with armor steel plates (image by R. Nüsing ISL). Right part: Flash X-ray cinematography used in terminal ballistic investigations. (Image by N. Faderl, R. Nüsing ISL)

[1] ISL: Institute of Saint Louis, 68301 SAINT LOUIS CEDEX, France

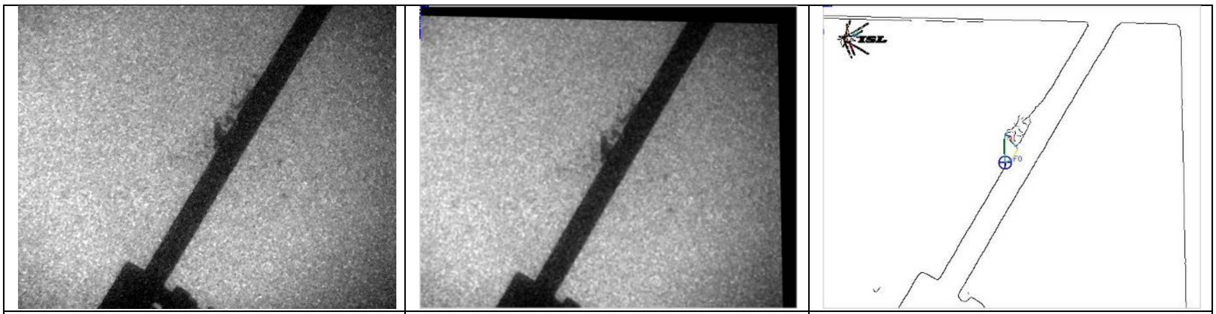

(a) Original image	(b) Aligned image	(c) Edge & Fragment Detection

Figure 3: Experimental post-processing: The images obtained with the multi-anode X-ray observation setup (a) have to be aligned first (b). In a second step (c), an edge detection algorithm is used to identify the fragments.

2.3 Experimental Results

In the experiment we can observe three different scenarios: For perpendicular impact, the surrogate perforates the plate and extrudes a plug. In the range between 15 and 60 degrees, we observe a broken ricochet. For larger angles, e.g.b *75* degrees, the ricochet stays intact.
In all experiments, the tip is fragmented, such that only one remaining part of significant size (> 1g) is found. For all angles, except for *75* degrees, the mass of this remainder is between *3.35g* and *4.78g* (*32% – 46%* of initial mass). The smallest mass is observed for 45 degrees, and the largest for 0 and 60 degrees.
This conference paper focusses on the two angles of 30 and 75 degrees: The quantitative evaluation of the experiments is shown in Table 1. The initial velocity varies between *781m/s* and *845m/s* and the yaw is acceptably low. For 30 degrees, the mass of the remainder varies slightly, whilst for the 75 degrees impact case, the erosion of the projectile is negligible with low variance (*3%*).
Figure 4 and Figure 5 show the qualitative behavior. For the broken ricochet (left image in Figure 4) we can only observe, that the interaction happens in a very small area, but the actual physical behavior remains hidden to the observer. The separate images depicted in Figure 5 can reveal exactly this. Each row shows one of the two experiments conducted at 30 degrees. From these images, we gain an insight into what is going on. The perforator hits the wall, the nose of it is eroded, the surrogate starts rotating, and it rebounds. We further observe how long the surrogate interacts with the wall (*60 - 80 µs*), that there is a counterclockwise rotation (*20.000 - 25.000 rad/s*) and a residual velocity perpendicular to the impact velocity (*150 - 300m/s*). The values have been extracted from the X-ray images and are given with a distinct uncertainty range due to the post-processing steps explained in Figure 3.

Experiment	***30° (#1)***	***30° (#2)***	***75° (#1)***	***75° (#2)***
Initial velocity	791 m/s (99% v_0)	781 m/s (98% v_0)	845 m/s (106% v_0)	785 m/s (98% v_0)
Yaw	-2.7°	+2.2°	+0.3°	-0.3°
Residual Mass	*3.62g (35% m_0)*	*4.08g (40% m_0)*	9.99g (97% m_0)	9.98g (97% m_0)

Table 1: Evaluation of the experiments. Extract for angles compared in this paper. The initial velocity is compared to the desired impact speed (v_0=800m/s). The residual mass is compared to the initial mass (m_0 =10.3g).

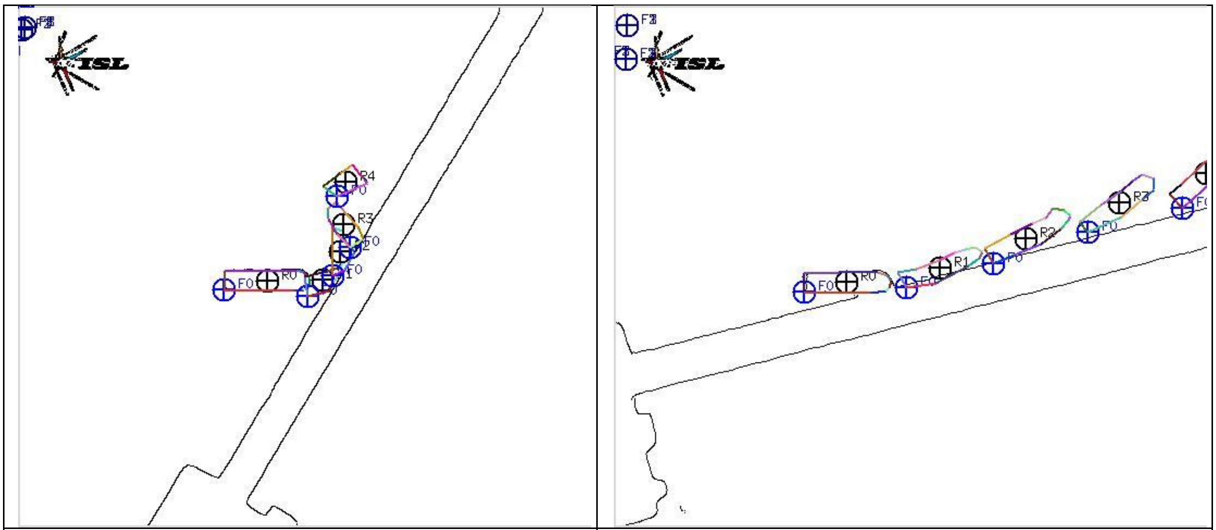

(a) 30 degrees impact: ricochet broken	(b) 75 degree impact: ricochet intact

Figure 4: The aligned images can be superposed to observe the dynamic behavior. For smaller angles (30 degrees (a)) these images do not reveal the behavior sufficiently. Instead, the separated images in Figure 5 have to be compared. For the angle of 75 degrees (b), we can observe the behavior. Further, one can measure the reflection angle and guess that the energy loss during an intact ricochet is negligible.

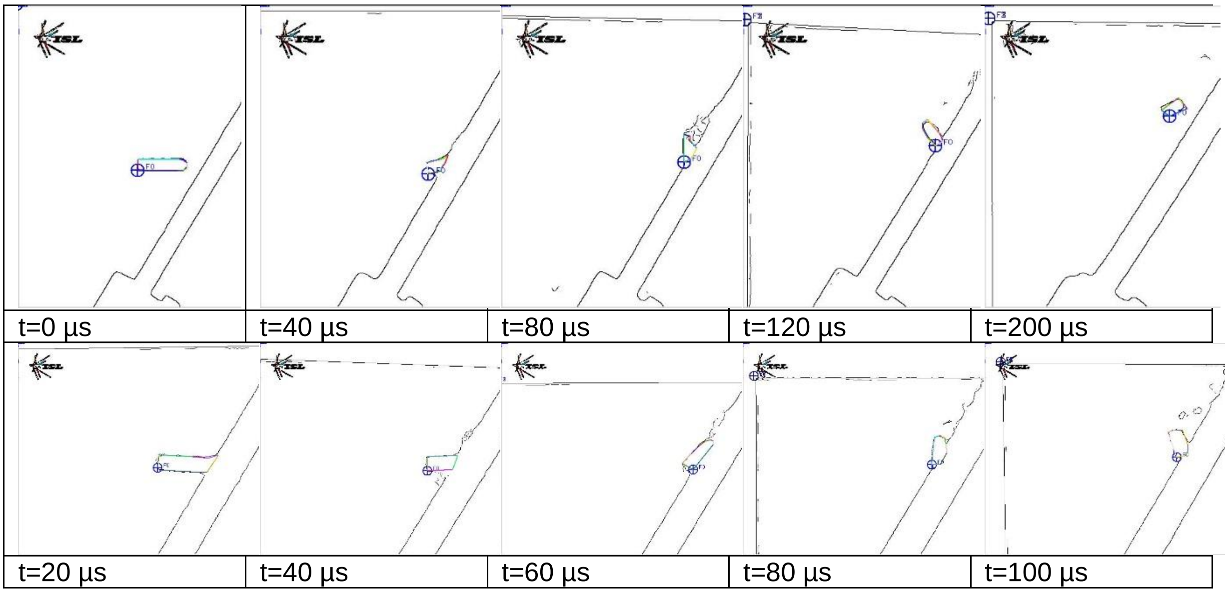

t=0 µs	t=40 µs	t=80 µs	t=120 µs	t=200 µs
t=20 µs	t=40 µs	t=60 µs	t=80 µs	t=100 µs

Figure 5: As pointed out in Figure 4, we need separate images to understand the dynamic behavior for the case of 30 degrees impact. The image matrix shows two different experiments in each row with the same setup, but different exposure times and different lenses. The behavior looks similar in subsequent experiments, and, thus, the experiment is qualitatively reproducible. For instance, the mass of the remainder is 10% larger in the second experiment and the rotational velocity, extracted from the X-ray images is of the same order of magnitude (20.000 and 25.000 rad/s).

3 Modeling

3.1 The Finite Element Method (FEM)

3.1.1 Description

The FEM is historically used in a lot of different applications. Due to a comprehensive theoretical background, there exists a broad knowledge of convergence properties, error bounds and limitations of the method. As the state-of-the-art method, we want to see how it performs for this particular application in comparison to the two particle-based methods SPH and SPG.

3.1.2 Meshing

We use a hexahedral mesh for the computation with the FEM. Instead of utilizing the meshing capabilities of LS-Prepost we developed an isolated meshing script for this simplified geometry. For the surrogate, it generates first the nodes of the half sphere at the tip of the projectile, and then extrudes a cylinder with a uniform spacing, similar to the inner-region of the sphere. This allows to quickly generate meshes of arbitrary resolution. For the target, we also propose our own meshing technique. The main challenge is that the target plate is very large compared to the area of impact. The resolution required outside the impact area is only of secondary importance, but there should be a smooth change in element size. Based on these requirements we developed an approach for a full FE-meshing (compare Figure 6) and also the meshing of only finite elements around a cylindrical hole which is then filled with SPH-particles providing a hybrid meshing (compare Figure 7).

3.1.3 Element Formulation/ Settings

Among those element formulations compared with LS-DYNA®, we achieved the best results with **`ELFORM=2`**. Thus we apply it to all FEM parts. Another possibility is formulation **`-1`** or **`-2`** which are recommended for large deformation and thin elements. Hourglassing is not activated as the element-formulation accounts for this issue using fully-integrated elements[2]. A good review of the different element formulation is done by Erhart [9]. Başaran [4] proposes **`ELFORM=0`** with hourglass **`HG_ID=10`**. Both, runtime and accuracy, were better with the fully integrated element.

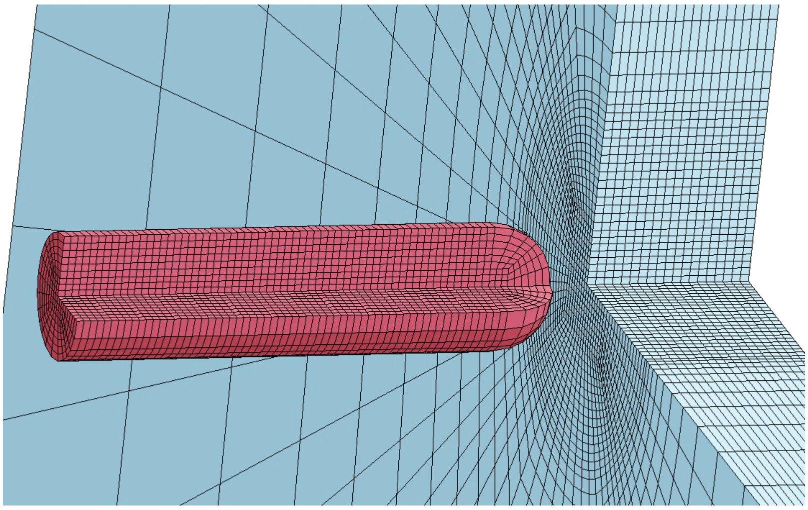

Figure 6: Meshing of the surrogate with hexahedral Lagrangian elements: This example shows the meshing with an element length of 0.4mm. The target consists of 44.000 elements, and the perforator requires 12.000 elements. A bias factor of approximately 1.4 is used in the butterfly setup of the target. The refined impact area of the target has three times the diameter of the perforator.

3.2 Smooth Particle Hydrodynamics (SPH)

3.2.1 Description

SPH [10] has its strength in particular for very high velocities and fluid applications [11, 12]. The behavior we are interested in lies between two velocity ranges. The first is the structural domain, where the strength of the material dominates the behavior (O(10m/s)). The second is the hydrodynamic domain, where the strength becomes irrelevant and instead the equation of state prescribes the behavior (O(1000m/s)). The structural application is well described with Lagrangian FEM and for the hypervelocity impact, SPH gives good results. The aim is not to describe the fluid-like behavior, as our application is below the critical velocity of hydrodynamics. We are interested in the fracture which is difficult to predict with mesh-based approaches. Thus, the SPH method seems to be a reasonable choice for our application.

[2] https://www.dynasupport.com/howtos/element/hourglass

3.2.2 Particle population

The particle distribution for the SPH method is generated with a self-written script to fulfill the quality requirements, to avoid numerical fracture, and to exclude unphysical behavior *[13]*. Further, it allows comparing differently refined setups to see whether the chosen resolution is already converged.

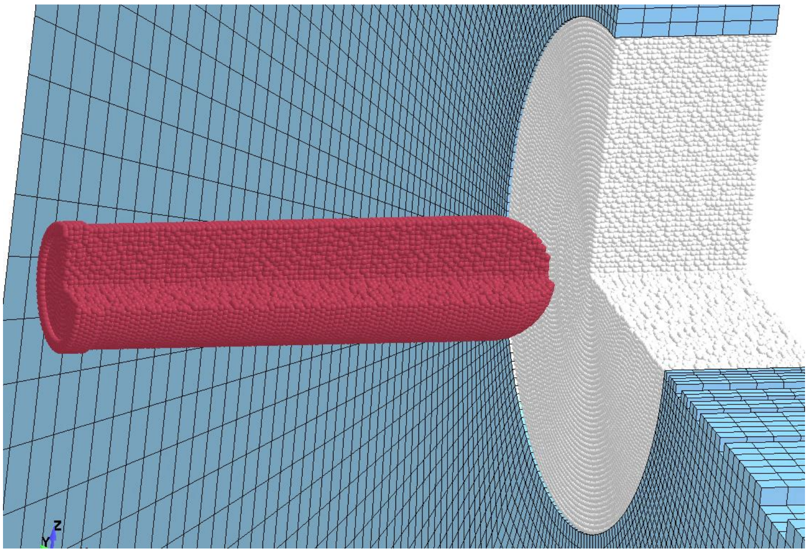

*Figure 7: Particle distribution for the SPH setup: The Lagrangian mesh around the impact area remains to reduce the runtime (cp. Figure 6). In the impact region, SPH particles are connected with a tied contact **CONTACT_TIED_NODES_TO_SURFACE_CONSTRAINED_OFFSET_MPP_ID** to the FEM. This setup consists of 55.000 particles for the surrogate and 240.000 particles for the target.*

3.2.3 Formulation/ Settings

LS-DYNA® offers the user different SPH-formulations and other SPH specific settings to tune the model. For our applications, three formulations are reasonable. The first is the standard SPH-formulation **IFORM=0**. The second formulation **IFORM=1** is more accurate but less stable. The third possibility is **IFORM=12**, which has been developed in the last few years by Yreux [14]. It is supposed to be more accurate by using slightly shifted integration points and thus achieving a quasi-linear reproducing property. However, it is not available in the commercial version up to now and requires an *mpp* setup. In this comparison, the renormalized formulation **IFORM=1** and **IFORM=12** are compared.
In addition to that, we choose the following settings: For faster computation, we use a **DEFINE_BOX** in the region where SPH particles need to be calculated. For stability and runtime reasons, we choose a cut-off velocity (**VMAX**) 20% larger than the impact speed. Further, we enable **IEROD=1**, and **ICONT=1**, to avoid any contact of eroded SPH particles.

3.3 Smooth Particle Galerkin (SPG)

3.3.1 Description

The Computational and Multi-scale Mechanics Group of LSTC (CMMG[3]) by Wu et al. works since several years on a better description of brittle and ductile failure in three different applications: Material Design, Manufacturing and Structural Analysis. The last application deals with low/medium and high-speed impact in different material, in particular steel. Thus, it is supposed to be a good choice for our application as well. They propose a particle-based method: SPG. It is beyond the scope of this paper to explain the theoretical background of it. Instead, the general ideas are recapitulated in the following: Similar to SPH, the weak form is integrated using direct nodal integration. However, here this technique uses a nonresidual penalty-type stabilization term derived from strain smoothing to obtain more stable and accurate results. Additionally, a bond-based failure mechanism is introduced to avoid self-healing of the material which is observed with other mesh-free approximations in the failure analysis. Different

[3] https://www.lstc-cmmg.org/

kernels have been implemented within this framework. For the high-velocity impact, the updated Lagrangian kernel is suggested by the developers [14].

3.3.2 Background Mesh

The SPG particle method was originally designed to simulate large deformations during material forming. Thus, most users already have a computational grid for their application and instead of providing a particle distribution in the input-deck, a background-mesh has to be defined. A hexahedral background mesh results in similar artifacts already observed with SPH [13]. Instead, a tetrahedral mesh is used for defining the particle positions.

3.3.3 Settings

There exist two options for using SPG: Either applying the implemented bond-based failure model (**`IDAM = 1`**) or stick to the failure model provided in the **`*MATERIAL`**-keyword. If the bond-based failure model is chosen the damage parameters have to be set to zero to avoid any interference.

3.4 Material and Failure Model

This paper uses the Johnson-Cook material model [15, 16] with material and failure parameters determined by ETH Zurich [3, 17]. The impactor and the target consist of the same armor steel. This reduces the uncertainties due to inaccurate material characterization. The keyword **`*MAT_ADD_EROSION`** is not used here. Additional to the material, the Grueneisen equation of state is obligatory.

3.5 Contact Definition

The **`CONTACT_ERODING_SURFACE_TO_SURFACE`** is used here for the FEM. It allows element erosion during the contact and has two applicable implementations. The standard contact type is penalty based (**`SOFT=0`**) and the other uses the “pinball”- algorithm (**`SOFT=2`**). The **`EROSOP`** flag allows contact of an eroded element and the **`IADJ`** flag allows the erosion not only for free boundaries but also on the boundary of the material subset. All other flags were set to default. Başaran [4] suggests to reduce the bucket sort frequency for the contact to **`BSORT=1`** for high-velocity impact to ensure correct contact detection. For **`SOFT=0,`** the contact was not correctly detected if the stiffness factor was smaller or equal one. Changing the bucket sort frequency does not solve this issue. Only an artificial increase of the stiffness factor to three or higher results in nonpenetrating material.

3.6 Target Response

3.6.1 Rigid Wall

To focus on the numerical approach and neglect effects from modeling the target, a **`RIGID_WALL`** formulation can be applied, instead of meshing the target. However, the steeper the impact angle, the less accurate is this assumption. For a convergence study, not presented in this paper, this simplification was applied to decrease the overall runtime.

3.6.2 Hybrid SPH-FEM Target

To quantify the influence of neglecting the actual target response there are two options. One option suggested by the authors is using a hybrid SPH-FEM description for the target [18] (compare Figure 7). In particular, for an SPH perforator, no Lagrangian elements are involved in the contact, and thus the timestep is not decreased due to highly deformed elements.

3.6.3 FEM Target

The most common description for the target response, is an FE block. The challenge here is to have a fixed mesh-size in the impact area, but still capture the boundary conditions correctly. In particular, the mesh-size in the direction of impact is important for correct contact detection. To achieve a reasonable runtime, a butterfly-like mesh is used which accounts for these requirements. The script generates a mesh with a user-defined mesh-size defined by only one parameter. Hence, less degrees of freedom have to be investigated, and a consistent mesh-refinement strategy for convergence studies is being developed.

4 Results

4.1 Comparison for a Broken Ricochet (30degrees NATO impact)

A broken ricochet is observed in the experiments for an impact angle of 30 degrees. In addition to this qualitative observation, we have a rough estimate for the residual velocity (*150 – 300m/s*), the rotational velocity (*15.000 – 25.000 rad/s*) and measured the mass of the remainder (*3.6 – 4.0g*). We are still in contact with SPG developers to determine a proper SPG setup, and therefore, focus on results obtained with FEM and SPH in this paper.

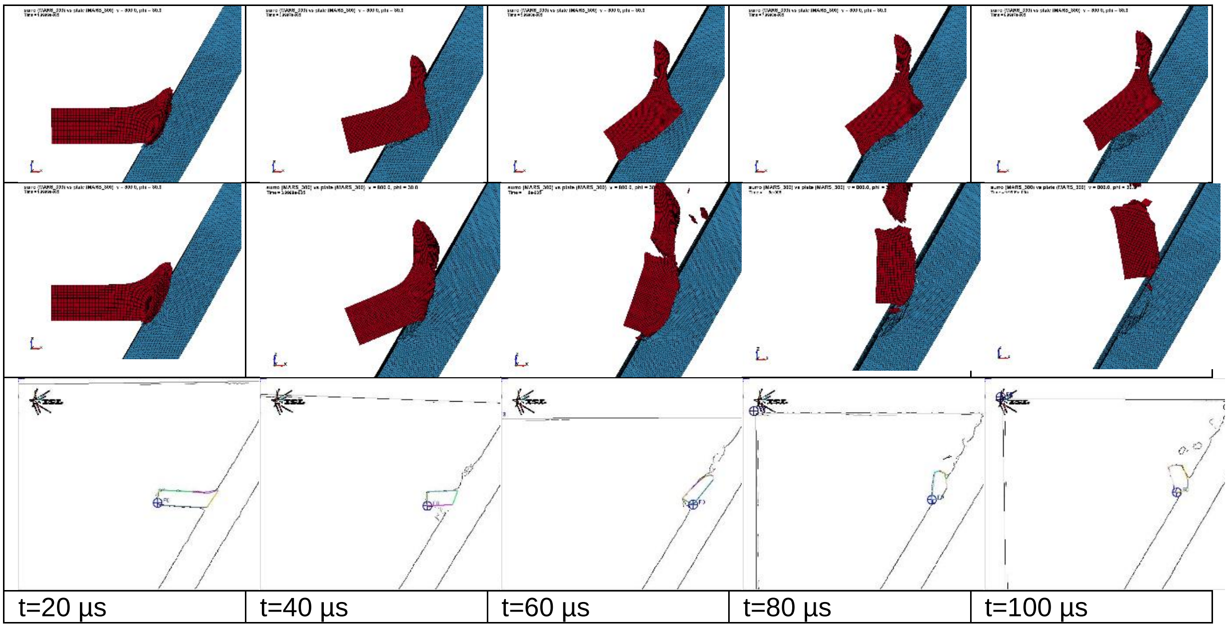

*Figure 8: Finite element simulation results for 30 degrees obliquity at 800m/s. First row **SOFT=0**, second row **SOFT=2**, last row: experiment. The penalty based contact formulation (**SOFT=0**) is not able to predict the fracture. If the pinball contact definition is used we observe similar behavior like in the experiment.*

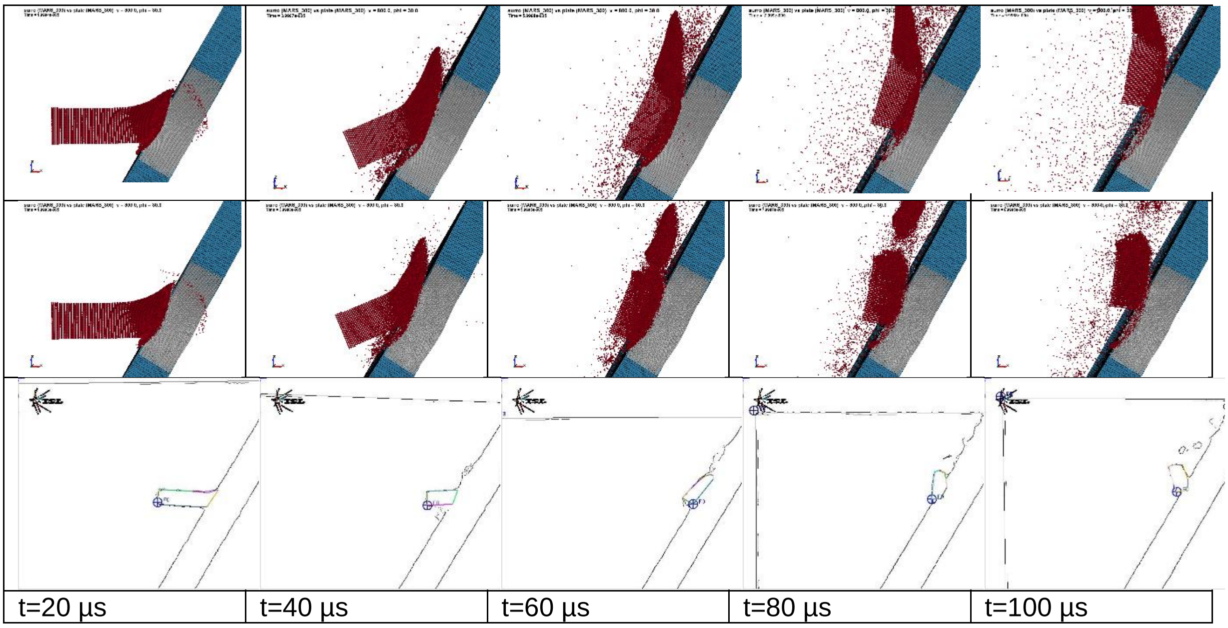

*Figure 9: Surrogate (SPH) against 30deg inclined plate (hybrid mesh) at 800m/s. First row: **FORM=12**, second row: **FORM=1**, third row: experiment. **FORM=12** does not predict a crack. **FORM=1** predicts the crack similar to the experiment. The rotation of the remainder is underpredicted by both methods.*

For an impact angle of 30 degrees, the behavior of the surrogate depends on the target response. For consistency, we compare the impact of the FE-surrogate against an FE-target and the SPH-surrogate against the hybrid SPH-FEM target. For the FEM the choice of the contact formulation has the most distinct influence on the result. Thus, Figure 8 compares the two contact implementations **`SOFT=0`** and **`SOFT=2`**. The standard contact formulation **`SOFT=0`** overpredicts the depth of penetration for the impact. This can be observed best for t=60µs. Hence, the surrogate does not ricochet off but gets stopped in the material. The pinball algorithm **`SOFT=2`** is qualitatively very similar to the experimental results. In particular, the last image for t=100µs is in very good agreement. The residual mass measures 5.3g (+13%) and the residual velocity of 256m/s is in good accordance, too. For the SPH-results, we present the differences between the renormalized formulation **`FORM=1`** and the new formulation of Yreux **`FORM=12`** in Figure 9. The new formulation does not predict the fracture, the renormalized formulation is in better accordance with the simulation results.

4.2 Comparison of an Intact Ricochet (75degrees NATO impact)

The second case investigates the intact ricochet which is observed for an oblique angle of 75 degrees. For this angle, the surrogate interacts much longer with the target such that in total 200µs are required for the comparison. The behavior observed in the experiment (compare Figure 10a) is a rebound of the projectile with slight bending and a very small deflection angle (3.6 degrees measured in the experiment). There is very little erosion at the penetrator (3% of total mass) and little loss of kinetic energy (27m/s decrease in velocity).
The Lagrangian FE (10b) is very well capable to predict this behavior. All properties observed in the experiment were reproduced. On the other hand, the SPH result (10c) overpredicts the energy loss during the impact. The surrogate is decelerated by 160m/s losing approximately 40% of his kinetic energy. The bending is underpredicted as well. The general behavior of the rebound without fracture can be reproduced with SPH, but the energy loss and bending is unacceptable.

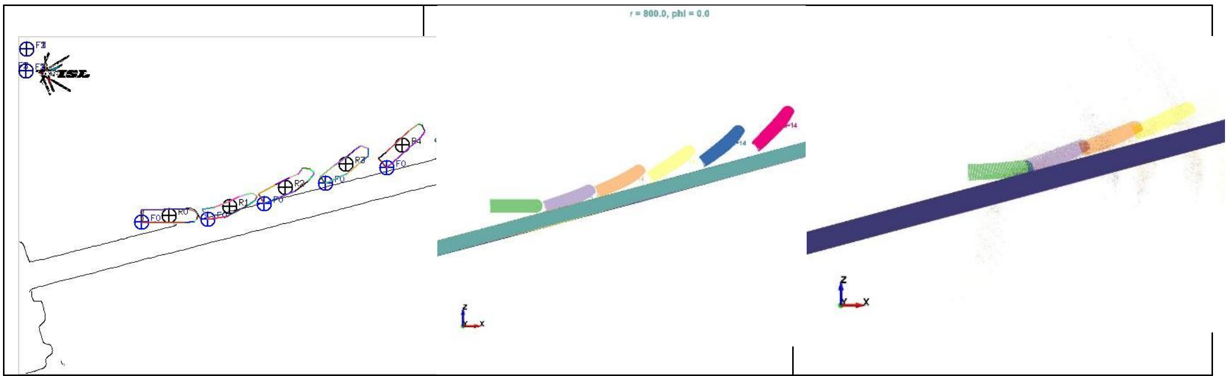

(a) Experiment (v^{loss}=29m/s) | (b) FEM result (v^{loss}=27m/s) | (c) SPH result (v^{loss}=158m/s)

Figure 10: Surrogate against 75deg inclined plate at 800m/s. First image: experiment, second image: FEM result, third image: SPG result. The colors visualize the dynamic behavior. The images are captured at an incremental timestep of 40 µs. v^{loss} is the difference between initial and residual velocity of the surrogate.

5 Summary and Conclusion

This paper presents an extract of the experiments which were conducted to validate numerical models during HVI. Different oblique angles are investigated and observed with X-ray cinematography. Besides comparing the qualitative behavior, we developed a software to extract quantitative values from the images. Thereby, we have a comprehensive database to compare our numerical experiments against.
The LS-DYNA® input decks were generated with a Python tool where all our experience in modeling HVI is incorporated. For instance, we already proposed an advanced method to generate a uniform particle distribution for the SPH parts [13]. For the target, we compare a hybrid FEM/SPH approach to a fully Lagrangian finite-element discretization. The region where the impact happens has a fixed resolution and the size is chosen according to the impact angle. Further, the tool keeps this transition smooth and generates keywords depending on the impact settings. As a result of that, we have a reproducible strategy in setting up the simulations and exclude any erroneous input by the user.

In addition, this paper proposes the following modeling approach. For the FE, we suggest the element type (**ELFORM=2**), and for the SPH formulation (**FORM=1**) of the conservative equations. For the material behavior, we use the Johnson-Cook material model (**MAT_ID=15**).
Although only small erosion at the target was observed during the experiment, a simplification of the target with a rigid wall is not advised. It changes the physical behavior of the contact too much and correlations are only found by accident. Instead, we suggest the fully FEM target for a Lagrangian impactor and the hybrid target for an SPH impactor.
Two different angles were investigated in this paper. The 30 degrees impact represents the case of broken ricochet and the 75 degrees impact an intact ricochet. The fracture behavior can be predicted with the SPH method using **FORM=1** and with FE with **SOFT=2**. On the other hand, the bending and rotation observed for the case of 75 degrees are better reproduced with the FEM.
Wu et al. show a large potential of the SPG method for penetration and perforation in their paper [6]. We ran tests with SPG but are still in contact with the developers about the best SPG setup for our application. Investigations on SPG and a comparison of the full range of obliquity will be part of an ongoing study.

Acknowledgements:

The authors acknowledge the contribution of the SPH and SPG developers from LSTC to the simulation setup in the paper. Further, they acknowledge the ISL for funding the work and the support of the University of Stuttgart and Lille University.

6 Literature

[1] M. Becker, "Numerical Ricochet Model of a 7.62 mm Projectile Penetrating an Armor Steel Plate," in *15th International LS-DYNA Users Conference*, 2018.

[2] V. Favorsky and e. al., Experimental-Numerical Study of Inclined Impact in Al7075-T7351 Targets by 0.3" AP Projectiles, US: 26th ISB, 2011.

[3] T. Fras, C. Roth and D. Mohr, "Fracture of high-strength armor steel under impact loading," *International Journal of Impact Engineering,* 2017.

[4] G. Basaran, "Numerical Study of High Velocity Impact Response of Vehicle Armor Combination Using LS DYNA(R)," Salzburg, 2017.

[5] N. Kilic and S. Bedir, "Ballistic behavior of high hardness perforated armor plates against 7.62 mm armor piercing projectile," *Materials and Design,* 2014.

[6] Y. W. a. C. T. Wu, "Simulation of Impact Penetration and Perforation of Metal Targets Using the Smoothed Particle Galerkin Method," *Journal of Engineering Mechanics,* vol. 8, 2018.

[7] J. Hallquist, "LS-DYNA Theory Manual," 2006.

[8] N. a. B. M. Faderl, "High-Speed 300keV flash X-ray cinematography for investigations of the ballistic impact behavior of target materials and structures," 2018.

[9] T. Erhart, "Review of Solid Element Formulations in LS-DYNA," LS-DYNA Forum 2011, Stuttgart, 2011.

[10] R. A. Gingold and J. J. Monaghan, "Smoothed particle hydrodynamics: theory and application to non-spherical stars," *Monthly notices of the royal astronomical society,* vol. 181, pp. 375-389, 1977.

[11] R. M. M. S. B. v. d. L. B. K. Iason Zisis, "Two-phase benchmarks for SPH multiphase fully compressible schemes," 2014.

[12] J. W. M. S. J Xu, "SPH and ALE formulations for sloshing tank analysis," *International Journal of Multiphysics,* vol. 9, no. 3, 2015.

[13] M. Becker, "A Study on Initial Conditions in Smooth-Particle-Hydrodynamics Modelling of High-Velocity-Impact," in *2018 Nordic LS-DYNA® Users Conference*, Sweden, Gothenburg, 2018.

[14] E. Yreux and J.-S. Chen, "A quasi-linear reproducing kernel particle method," *International Journal for Numerical Methods in Engineering,* vol. 109, pp. 1045-1064, 2017.

[15] G. C. W. Johnson, "A constitutive model and data for metals subjected to large strains, high strain rates and high temperatures," *Proceedings of the Seventh International Symposium on Ballistics.,* 1983.

[16] G. C. W. Johnson, "Fracture characteristics of three metals subjected tovarious strains, strain rates, temperatures and pressures.," *Engineering Fracture Mechanics,* vol. 21, no. 1, 1985.

[17] T. e. a. Fras, "Strikers with different nose shape impacting an armor steel - numerical modelling," Proceedings 12th European LS-DYNA Conference 2019, Koblenz, Germany, 2019.

[18] M. Becker, "Automatic Mesh-Generation (FEM/SPH) for HVI-Simulations of Arbitrary Rotational Symmetric Impactors," Procedings of HVIS 2019, Destin, Florida, 2019.

[19] P. Diehl, "Modeling and Simulation of cracks and fractures with peridynamics in brittle materials," 2017.